

<Original Papers>Effects of Interleukin-3 on Diaphragm Muscle Contraction in a Septic Animal Model

著者	ARAKI Hirofumi, SHINDOH Chiyohiko, SHINDOH Yuriko, SHIRATO Kunio
journal or publication title	東北大学医療技術短期大学部紀要 = Bulletin of College of Medical Sciences, Tohoku University
volume	11
number	2
page range	151-163
year	2002-07-31
URL	http://hdl.handle.net/10097/33789

Effects of Interleukin-3 on Diaphragm Muscle Contraction in a Septic Animal Model

Hirofumi ARAKI, Chiyohiko SHINDOH, Yuriko SHINDOH* and Kunio SHIRATO**

Department of Medical Technology, College of Medical Sciences, Tohoku University

**Department of Respiratory Medicine, Sendai City Medical Center*

***First Department of Internal Medicine, Tohoku University School of Medicine*

敗血症動物モデルにおける横隔膜筋収縮への IL-3 の影響

荒木宏文, 進藤千代彦, 進藤百合子*, 白土邦男**

東北大学医療技術短期大学部 衛生技術学科

*仙台市医療センター 呼吸器内科

**東北大学大学院医学系研究科 循環器病態分野

Key words: Endotoxin, IL-3, NADPH diaphorase, nitric oxide, superoxide

Interleukin-3 (IL-3) is one of a number of colony stimulating factors which are known to regulate hematopoiesis and cell death (apoptosis). In the present study, however, we examined another possible function of IL-3, namely, whether it affects diaphragm contractile properties in rats. In the saline+endotoxin group, the force-frequency curves decreased significantly at 4 hours (1.63 ± 0.06 kg/cm², $p < 0.05$) from those at 0 hours (1.84 ± 0.07 kg/cm²); muscle fibers which showed increased NADPH diaphorase staining were types I (SO) and IIa (FOG). In the IL-3+endotoxin group, the force-frequency curves did not show significant changes between 0 hours (1.72 ± 0.15 kg/cm²) and 4 hours (1.70 ± 0.05 kg/cm²). In the IL-3 only group, the force-frequency curves at 4 hours (1.78 ± 0.10 kg/cm², $p < 0.05$) decreased significantly from those at 0 hours (2.12 ± 0.06 kg/cm²); muscle fibers which showed increased NADPH diaphorase staining were also types I (SO) and type IIa (FOG). IL-3 itself significantly decreased force-frequency curves and induced NO production in the diaphragm muscle fibers at 4 hours. From these results, IL-3 prevented the deterioration in force-frequency curves and NO production induced by endotoxin administration, therefore, it is suggested that IL-3 has a cell protecting effect coexisted with endotoxin.

Introduction

Interleukin-3 (IL-3) is one of a number of colony stimulating factors which are known to regulate haematopoiesis, and its cDNA sequence has been reported¹⁾. IL-3 is primarily produced by activated T cells and has vari-

ous functions: It stimulates colony formation of multiple lineages (multi-CSF) and maintains spleen colony forming units (CFU-S)²⁾³⁾, it serves as a growth factor for megakaryocytes⁴⁾, and it acts on pre-B cells⁵⁾ and on pre-T cells⁶⁾. Therefore, IL-3 is classified as a cytokine that has both activities of Th1 (helper T cell 1) and

Th2 (helper T cell 2) inductions⁷⁾.

IL-3 is also known to have another function, that is, IL-3 gene expression within tumors leading to host-cell infiltration, particularly by macrophages, slower tumor growth, and enhanced immunogenicity. TNF- α and NO are cytotoxic for a nonimmunogenic spontaneous fibrosarcoma (FSAN) cell line⁸⁾. IL-3 also plays a role in prolonging tissue leukocyte infiltration in a chronic maintained bronchial hyperresponsive mouse model by limiting clearance by apoptosis⁹⁾, and IL-3 or IL-2 induces apoptosis in the absence of serum (Bcl-2 protein). However, IL-3 or IL-2 with serum (Bcl-2 protein) has been shown to prevent cell death by apoptosis, either directly or by sensitizing cells to survival factors present in the serum¹⁰⁾. The increase of IL-3 induces *Bcl-2* mRNA and prevents apoptosis, while the decrease of IL-3 blocks *Bcl-2* mRNA induction and leads to apoptosis¹¹⁾. We have recently reported that IL-12 itself has an adverse effect on diaphragm muscle but that the combination of IL-12 and endotoxin can prevent the deteriorative effect of endotoxin only¹²⁾. This combination has also been found to prevent NO production detected as NADPH diaphorase staining.

Combining the previous reports mentioned above and our recent results, we hypothesized that IL-3 could have a protective effect against endotoxin-induced diaphragm muscle deterioration. We therefore examined the effects of the administration of a combination of IL-3 and endotoxin as well as the effects of IL-3 per se on diaphragm contractile properties in an endotoxin-induced diaphragm muscle deterioration model and performed NADPH diaphorase staining to detect NO production in the diaphragm muscle.

Methods

Animal preparation

Experiments were performed using 36 Wistar rats weighing 170.1 ± 4.3 g (Charles River Japan, Kanagawa, Japan) after receiving written approval from The Tohoku University Animal Facility. We tested the effects of IL-3 on diaphragm muscle in three groups. Group 1, the saline+endotoxin group ($n=12$), was given 0.5 ml of saline intravenously via the tail vein, followed by an intraperitoneal injection of *E. coli* endotoxin (30 mg/kg, 055: B5, Sigma Chemical Co., St. Louis, USA) in 0.5 ml of saline 5 minutes later. Group 2, the IL-3+endotoxin group ($n=12$), was given recombinant human IL-3 (0.25 μ g, B001-5, Medical & Biological Laboratories (MBL) Co., LTD., Nagoya) suspended in 0.5 ml of saline intravenously via the tail vein, followed by an intraperitoneal injection of *E. coli* endotoxin (30 mg/kg) in 0.5 ml of saline 5 minutes later. Group 3, the IL-3 only group ($n=12$), was given only recombinant human IL-3 (0.25 μ g, B001-5, MBL Co., LTD., Nagoya) suspended in 0.5 ml of saline intravenously via the tail vein. We measured force-frequency curves, twitch kinetics and fatigability at 0 hours and 4 hours in each group ($n=6$, respectively).

Diaphragm muscle contractile measurements

The measurements of diaphragm muscle contractility were performed as previously reported¹³⁾. Briefly, two muscle strips (3-4 mm wide) were dissected from the right and left hemidiaphragm under diethyl ether anesthesia and mounted in separate organ baths containing Krebs-Henseleit solution oxygenated with a 95% O₂-5% CO₂ gas mixture. The organ baths were heated in a water bath ($37 \pm 0.5^\circ\text{C}$, pH 7.40 ± 0.05). The composition of the aerated Krebs-Henseleit solution in mEq/L was as

follows: Na^+ , 153.8; K^+ , 5.0; Ca^{2+} , 5.0; Mg^{2+} , 2.0; Cl^- , 145.0; HCO_3^- , 15.0; HPO_4^{2-} , 1.9; SO_4^{2-} , 2.0; glucose, 110 mg%; $10 \mu\text{M}$ d-tubocurarine; regular crystalline zinc insulin, 50 U/L. Both muscle strips were simultaneously stimulated with supramaximal currents (i.e., 1.2 to 1.5 times the current required to elicit maximal twitch tension, 200–250 mA, 0.2 ms duration in pulses) by a constant current stimulus isolation unit (SS-302J, Nihon Kohden) driven by a stimulator (SEN-3201, Nihon Kohden). The elicited tensions were measured by a force transducer (UL-100GR, Minebea Co.). The length of each muscle strip was changed by moving the position of the force transducer with a micrometer-controlled rack and pinion gear (accuracy of displacement, 0.05 mm), and measured with a micrometer in close proximity to the muscle. The optimal length of the muscle (L_0) was defined as the muscle length at which twitch tension development was maximal, and this L_0 was maintained in the following measurements.

The diaphragm force-frequency relationship was assessed by sequentially stimulating muscles at 1, 10, 20, 30, 50, 70, 100 and 120 Hz. Each stimulus train was applied for approximately 1 second, and adjacent trains were applied at approximately 10-second intervals. The tensions of both muscle strips were recorded by a hot-pen recorder (RECTI-HORIZ-8K, San-ei).

Twitch contraction was elicited by a single pulse stimulation (0.2-millisecond duration of pulses), and the trace of the twitch contraction was recorded at high speed (10 cm/second). The twitch kinetics were assessed by (I) twitch tension (TT: peak tension of twitch contraction, kg/cm²), (II) contraction time (CT: the time required to develop peak tension, milliseconds) and (III) half-relaxation time (RT:

the time required for peak tension to fall by 50%, milliseconds) during a single muscle contraction. For analysis of the contractile velocity of twitch contractions, TT/CT (slope during contraction time) and (1/2 TT)/RT (slope during half-relaxation time) were calculated from the curve of the twitch contraction trace.

Muscle fatigability was then assessed by examining the rate of fall of tension over a 5-minute period of rhythmic contraction. Rhythmic contraction was induced by applying trains of 20 Hz stimuli (train duration, 0.3 seconds; rest duration, 0.7 seconds) at a rate of 60 trains/min. Muscle fatigability was expressed as a percentage of the final remaining tension (%) from the initial tension. After completion of this protocol, muscle strips were removed from the bath and weighed.

NADPH diaphorase staining

NADPH diaphorase histochemistry was performed at 0 and 4 hours in each group. After excision of the muscle strips mentioned above, the near diaphragm was quickly excised, and the tissue pieces were immersed in 2% paraformaldehyde in PB at 4°C for 12 hours, and then stored in 10% sucrose containing PB for cryoprotection at 4°C for at least 24 hours. Cryosections (10 μm in thickness) were cut from the diaphragm, mounted on chrome-alum gelatin-coated glass slides, and then immersed in 0.3% Triton X-100 containing phosphate buffer for histochemistry. The histochemical reaction for NADPH diaphorase was investigated by dipping the sections in 1.0 mM of freshly prepared β -NADPH (Oriental Yeast Co., LTD., Tokyo, Japan) and 0.2 mM nitroblue tetrazolium (Wako Pharmaceutical Co., Osaka, Japan) in 100 mM Tris-HCl buffer (pH 8.0) containing 0.2% Triton X-100 for 60 min at 37°C¹⁴. The reaction was stopped by rinsing the sections in PBS. The sections were cov-

ered with a mixture of glycerol and PBS (2:1) and photographed with an Olympus microscope using color reversal film (Sensia II, Fuji Film, Tokyo).

ATPase staining

Myofibrillar ATPase staining was performed according to the method of Dubowitz and Brooke¹⁵. The muscle strips in each group were adjusted to Lo with pins on a cork plate, immersed in isopentane (Wako Pure Chemical Industries Ltd.) that had been cooled in liquid nitrogen, and embedded in mounting medium (OCT compound, Miles Inc.). Diaphragm sample tissues were sectioned at 10 μm into sequential slices with a cryostat (BRIGHT Instrument) kept at -20°C . On the basis of their staining reactions for myofibrillar ATPase after alkaline (pH 10.4) and acid (pH 4.2 and 4.6) preincubation, muscle fibers were classified as either type I (slow-twitch and oxidative, SO) or type II subtypes, namely, IIa (fast-twitch, oxidative and glycolytic, FOG), IIb (fast-twitch and glycolytic, FG) and IIc (intermediate). This nomenclature is used as described by Dubowitz and Brooke¹⁵. With preincubation at a pH of 10.4, non-stained fibers were classified as type I, and dark stained fibers were classified as type II (IIa, IIb and IIc) muscle fiber. With preincubation at a pH of 4.2, non-stained fibers were classified as types IIa and IIb, and dark stained fibers were classified as type I and IIc muscle fiber; at a pH of 4.6, non-stained fibers were classified as type IIa, and dark stained fibers were classified as type I, IIb and IIc muscle fiber. The sections were mounted in artificial resin and photographed with an Olympus microscope using color reversal film (Sensia II, Fuji Film, Tokyo).

Data Analysis

The cross-sectional area of the strip was calculated by dividing the muscle mass by the

product of the length of the muscle and its density (1.06 g/cm^3)¹⁶, and tension was calculated as force per unit area (kg/cm^2). Data obtained from both halves of the diaphragm in one animal were averaged. The sample number used was $n=6$ (animals) per treatment/time point for force-frequency curves, twitch kinetics and fatigability. The mean values of tensions for each frequency in force-frequency

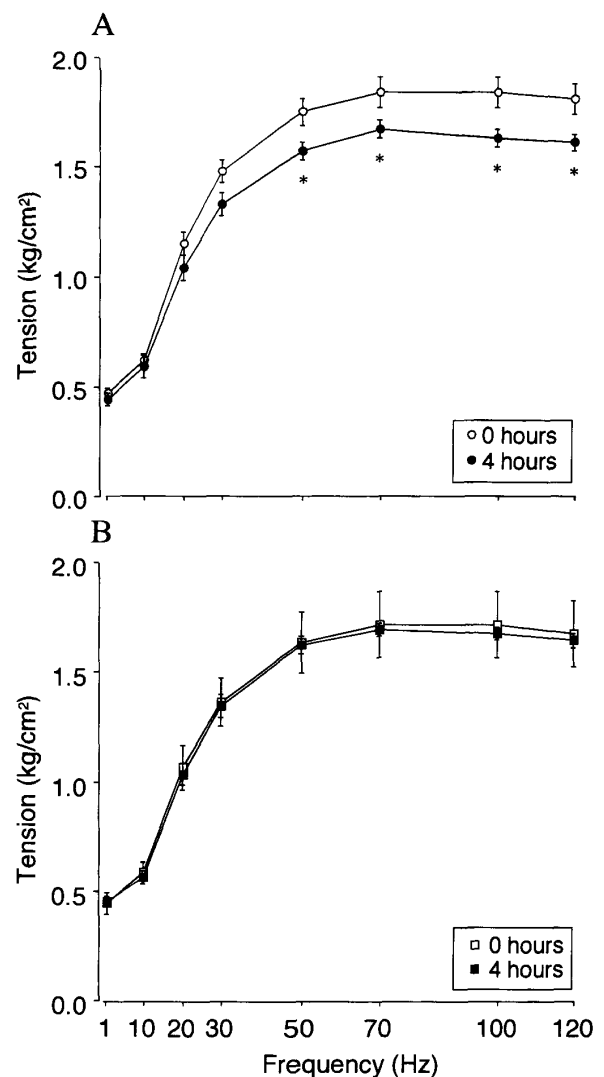


Fig. 1. Force-frequency curves of the saline+endotoxin group at 0 and 4 hours (A), and those of the IL-3+endotoxin group at 0 and 4 hours (B). Symbols indicate significant differences at given frequencies compared to 0 hours ($*p<0.05$).

curves, twitch kinetics and fatigability were compared by Student's *t*-test. To compare the entire configuration of each force-frequency curve at 0 and 4 hours of each group, analysis of variance (ANOVA) with Fisher's PLSD (Protected Least Significant Difference) *post hoc* test was performed. Data are presented as means \pm SE (standard error). Comparisons with a *p*-value of less than 0.05 were considered to be statistically significant.

Results

Changes of contractile properties in the saline + endotoxin and IL-3 + endotoxin groups

The force-frequency curves of the saline +

endotoxin group were obtained at 0 and 4 hours after intravenous injections of saline, followed by intraperitoneal injections of endotoxin (30 mg/kg) (Fig. 1A). The force-frequency curves to at 4 hours (1.63 ± 0.06 kg/cm² as a peak, $p < 0.05$) were significantly decreased from those at 0 hours (1.84 ± 0.07 kg/cm² as a peak), and there were significant decreases of tensions at from 50 to 120 Hz at 4 hours ($p < 0.05$ each) from those at 0 hours. Comparisons of whole force-frequency curves in each group were performed with ANOVA and Fisher's *post hoc* test; the force-frequency curves between 0 and 4 hours, however, did not significantly differ.

The force-frequency curves of the IL-3 + endotoxin group were obtained at 0 and 4 hours

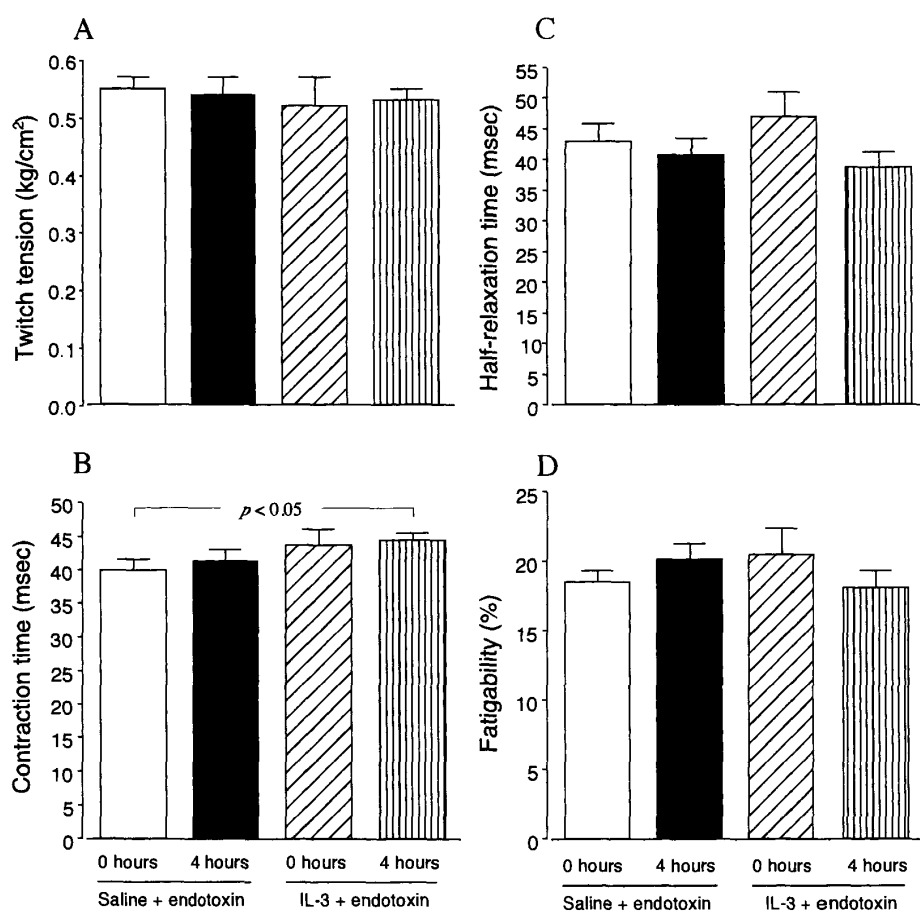


Fig. 2. Changes of twitch kinetics at 0 hours and 4 hours in the saline + endotoxin and IL-3 + endotoxin groups. A: twitch tension, B: contraction time, C: half-relaxation time, D: fatigability.

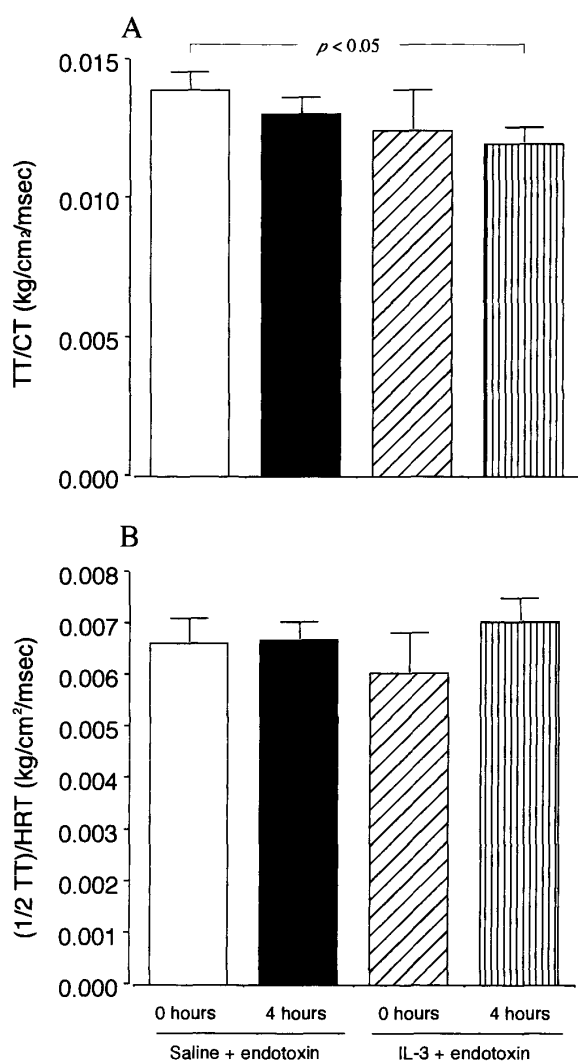


Fig. 3. Changes of TT/CT (A) and (1/2 TT)/HRT (B) at 0 hours and 4 hours in the saline+endotoxin and IL-3+endotoxin groups.

after injection of IL-3 intravenously followed by intraperitoneal injection of endotoxin (30 mg/kg) (Fig. 1B). There were no significant changes in frequency between 0 hours (1.72 ± 0.15 kg/cm² as a peak) and 4 hours (1.70 ± 0.05 kg/cm² as a peak) as shown by both Student's *t*-test and ANOVA. This indicates that IL-3 prevented the decrease of the force-frequency curves induced by endotoxin.

There were no significant changes in twitch tension (Fig. 2A), half-relaxation time (Fig. 2C) and fatigability (Fig. 2D) between 0 hours and 4

hours in the saline+endotoxin and IL-3+endotoxin groups. There was only a significant difference in contraction time (Fig. 2B) between 0 hours of the saline+endotoxin group and 4 hours of the IL-3+endotoxin group ($p < 0.05$).

There were no significant differences of TT/CT (Fig. 3A) and (1/2 TT)/HRT (Fig. 3B) between 0 hours and 4 hours in the saline+endotoxin and IL-3+endotoxin groups, except for a significant change of TT/CT between 0 hours of the saline+endotoxin group and 4 hours of the IL-3+endotoxin group ($p < 0.05$). In short, IL-3 in coexistence with endotoxin had a preventive effect on force-frequency curves, but only a slight effect on twitch kinetics.

NADPH diaphorase and ATPase stainings in the saline+endotoxin and IL-3+endotoxin groups

NADPH diaphorase staining was performed on diaphragm tissue at 0 hours (Fig. 4A) and 4 hours (Fig. 4B) in the saline+endotoxin group and at 0 hours (Fig. 4C) and 4 hours (Fig. 4D) in the IL-3+endotoxin group. At 0 hours in the saline+endotoxin group (Fig. 4A), there was very little staining of the muscle fibers, but some muscle fibers at 4 hours (Fig. 4B) showed relatively slight but darker staining (black arrows) compared with that at 0 hours. This enhanced staining seems to indicate increased NO production in the muscle fibers due to endotoxin. In the IL-3+endotoxin group, muscle fibers at 0 hours (Fig. 4C) and 4 hours (Fig. 4D) were similarly stained.

In the comparison of NADPH diaphorase staining at 0 hours (Fig. 5A) and 4 hours (Fig. 5B) in the saline+endotoxin group, the muscle fibers with increased NADPH diaphorase staining in Fig. 5B were identified as type I (SO) and type IIa (FOG) muscle fibers by ATPase staining at pH 10.4 (Fig. 5C) and at pH 4.6 (Fig. 5D).

IL-3 Effect on Diaphragm Muscle

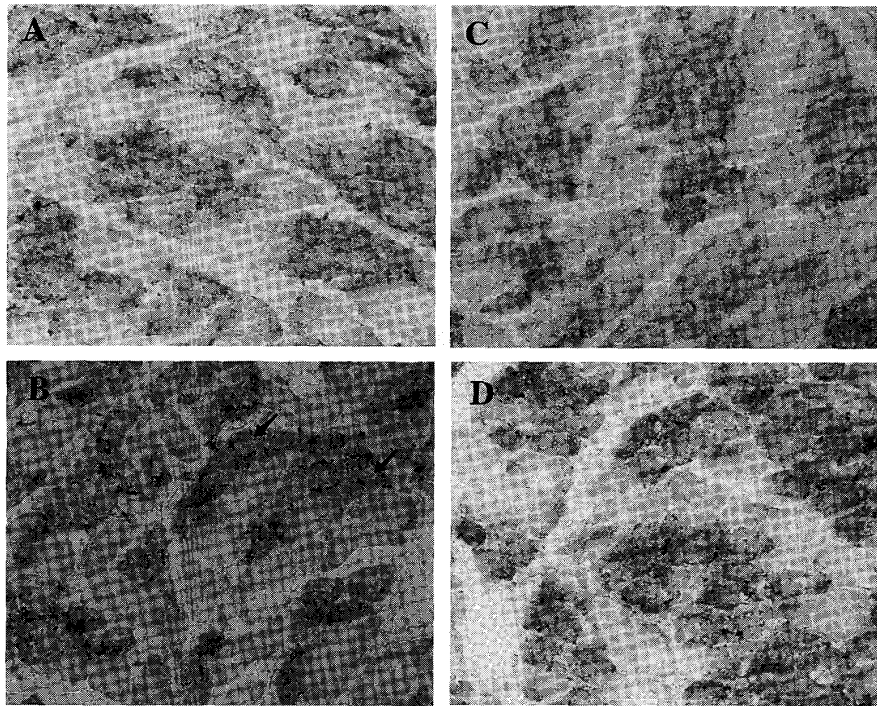


Fig. 4. NADPH diaphorase staining at 0 hours (A) and 4 hours (B) in the saline+endotoxin group, and at 0 hours (C) and 4 hours (D) in the IL-3+endotoxin group. Black arrows in (B) indicated the muscle fibers with increased staining.

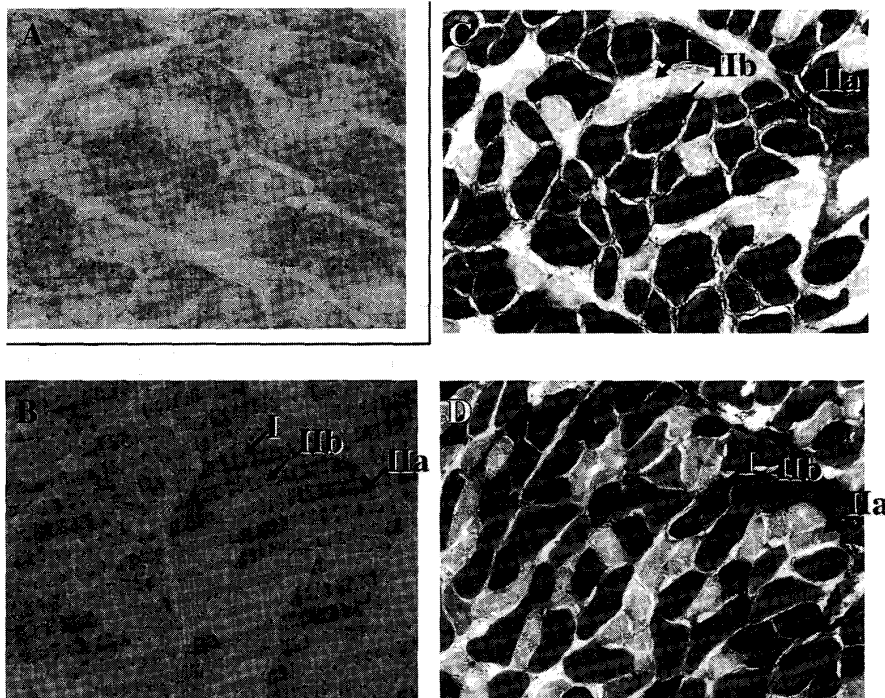


Fig. 5. NADPH diaphorase staining at 0 hours (A) and 4 hours (B), and ATPase staining at pH 10.4 (C), pH 4.6 (D) in the saline+endotoxin group. The muscle fibers with increased staining in (B) were identified as types I and IIa.

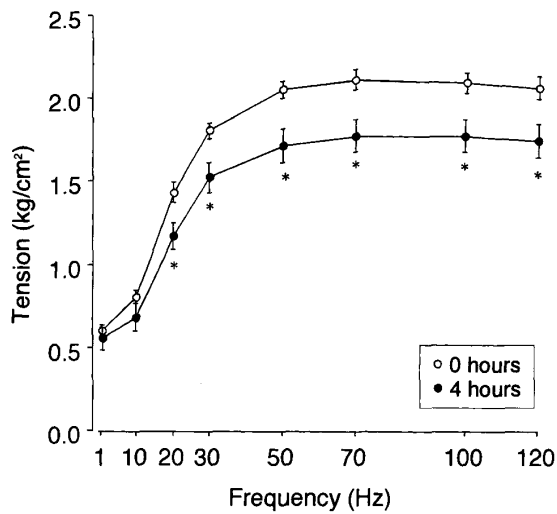


Fig. 6. Force-frequency curves of the IL-3 only group at 0 and 4 hours. Symbols indicate significant differences at given frequencies compared to 0 hours (* $p < 0.05$).

Changes of contractile properties in the IL-3 only group

The force-frequency curves of the IL-3 only group were obtained at 0 and 4 hours after intravenous injections of IL-3 (0.25 μg) (Fig. 6). The force-frequency curves at 4 hours ($1.78 \pm 0.10 \text{ kg/cm}^2$ as a peak, $p < 0.05$) were significantly lower than those at 0 hours ($2.12 \pm 0.06 \text{ kg/cm}^2$ as a peak), and there were significant decreases of tensions from 20 to 120 Hz at 4 hours ($p < 0.05$ each) from those at 0 hours. The force-frequency curves between 0 and 4 hours differed significantly ($p < 0.05$) by ANOVA.

There were no significant changes in twitch tension (Fig. 7A), contraction time (Fig. 7B), half-relaxation time (Fig. 7C), fatigability (Fig. 7D), TT/CT (Fig. 7E) and (1/2 TT)/HRT (Fig. 7F) between 0 hours and 4 hours in the IL-3 only group. In short, it was indicated that IL-3 per se had a deteriorative effect on force-frequency curves, but did not have a significant effect on twitch kinetics.

NADPH diaphorase and ATPase stainings in the IL-3 only group

In the comparison of NADPH diaphorase staining at 0 hours (Fig. 8A) and 4 hours (Fig. 8B) in the IL-3 only group, the muscle fibers with increased NADPH diaphorase staining in Fig. 8B were identified as type I (SO) and type IIa (FOG) muscle fibers by ATPase staining at pH 10.4 (Fig. 8C), pH 4.6 (Fig. 8D) and pH 4.2 (Fig. 8E). This indicates that IL-3 per se causes NO production in the diaphragm muscle fibers at 4 hours after its injection.

Discussion

Results of this study indicated that IL-3 itself caused significant decreases in force-frequency curves and that NO production in the diaphragm muscle fibers was induced 4 hours after intravenous injection of IL-3, as shown by NADPH diaphorase staining. However, the combination of IL-3 and endotoxin had no significant effects on force-frequency curves and twitch kinetics, while there was a significant decrease of force-frequency curves in the saline+endotoxin group. From these results, it is concluded that the deterioration in force-frequency curves and NO production induced by endotoxin administration is blocked by IL-3.

NADPH diaphorase staining showed that the production of NO and/or superoxide increased at 4 hours by the IL-3 only group and in the saline+endotoxin group. It is known that NO synthase activity occurs in the fatigued diaphragm muscle¹⁷⁾ and that NO production in the diaphragm muscle fibers is closely related to the inhibition of complex I (NADH: ubiquinone oxidoreductase) and complex II (succinate: ubiquinone oxidoreductase) activities of the mitochondrial respiratory chain. This NO-dependent inhibition might switch to anaer-

IL-3 Effect on Diaphragm Muscle

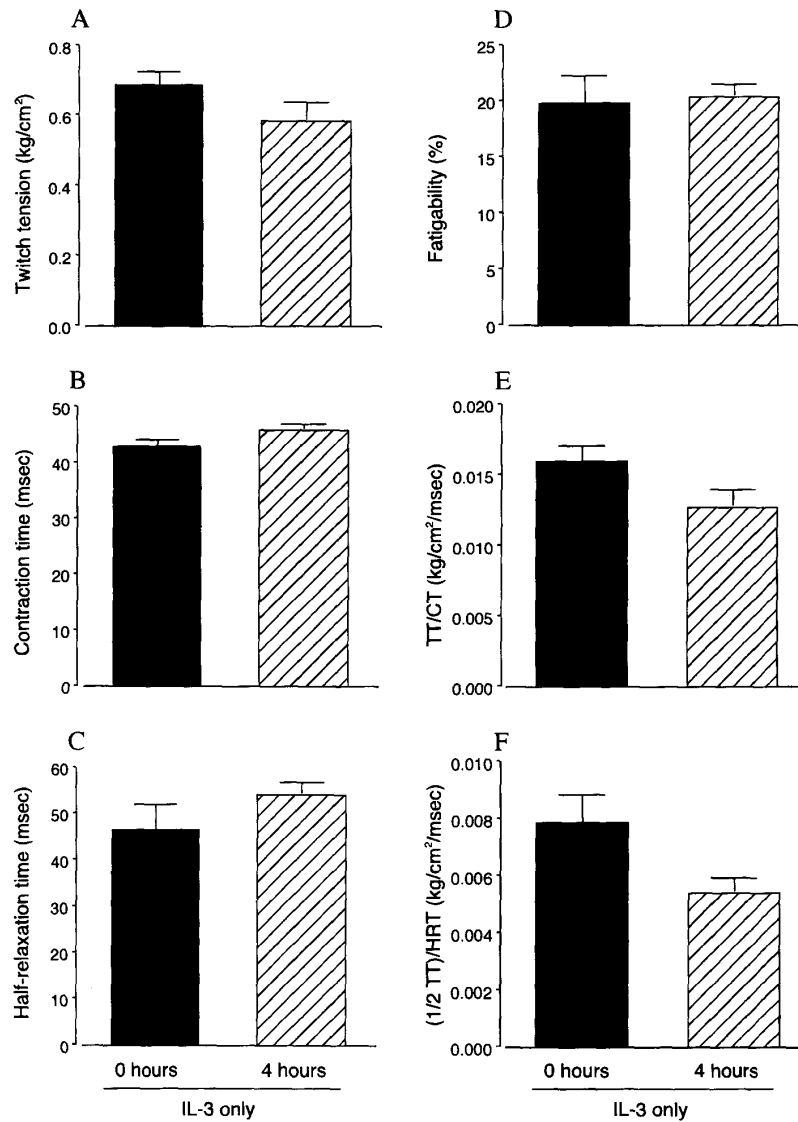


Fig. 7. Twitch kinetics in the IL-3 only group. A: twitch tension, B: contraction time, C: half-relaxation time, D, fatigability, E: TT/CT, F: (1/2 TT)/HRT.

obic glycolysis and reduce the energy production of the smooth muscle cells¹⁸). It is therefore likely that NO-dependent inhibition of mitochondrial respiration in diaphragm muscle cells is also responsible for the decrement of force-frequency curves.

At first, IL-3 has been primarily considered a stimulator of hematopoietic precursors, granulocytes, and mast cells²), and have established unique roles for antigen-specific T- and B-cell responses¹⁹). It has also been reported

that IL-3, unlike IL-2, works to generate cytotoxic effectors by a mechanism that requires CD4⁺ cells²⁰).

At second, the relationships of IL-3, Bcl-2 protein and cytochrome C have been clarified and involved in the signal transduction of apoptosis. An overexpression of *Bcl-2* mRNA is associated with the suppression of apoptosis in hemopoietic cells both *in vivo* and *in vitro*²¹). On the other hand, a withdrawal of IL-3 from the human factor-dependent eryth-

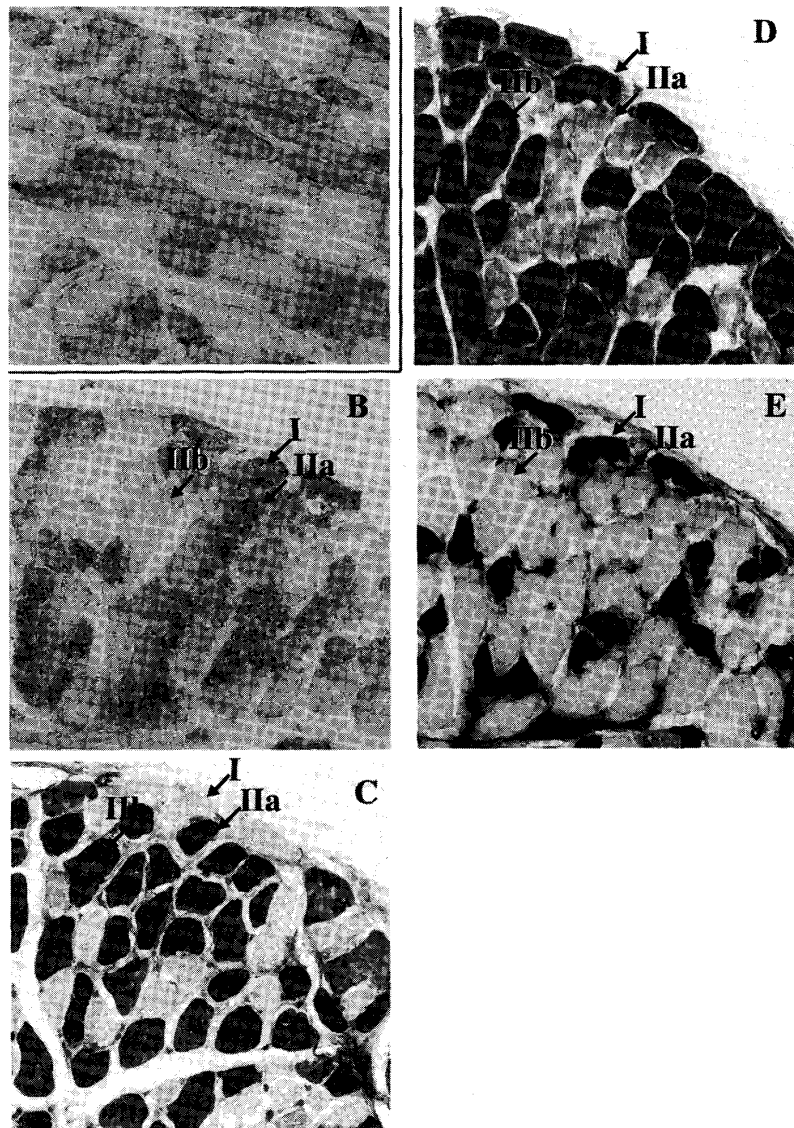


Fig. 8. NADPH diaphorase staining at 0 hours (A) and 4 hours (B), and ATPase staining at pH 10.4 (C), pH 4.6 (D) and pH 4.2 (E) in the IL-3 only group. The muscle fibers with increased staining in (B) were identified as types I and IIa.

roleukemic cell line TF-1 results in a decrease of *Bcl-2* mRNA and is accompanied by the onset of apoptosis as determined by flow cytometric analysis of DNA degradation¹¹). In a cell-free apoptosis system, it was found that mitochondria spontaneously released cytochrome C, which activated DEVD-specific caspases, leading apoptotic nuclear morphology. Therefore, *Bcl-2* acts on mitochondria to prevent the release of cytochrome C, thus

preventing caspase activation and the apoptotic process²²).

At third, concerning the antioxidant activity of IL-3, it has been reported that *Bcl-2* is localized in mitochondria, the endoplasmic reticulum and nuclear membranes, as well as the sites of reactive oxygen species generation. *Bcl-2* does not appear to influence the generation of oxygen free radicals, but does prevent oxidative damage to cellular constituents in-

cluding lipid membranes, i.e., it blocks peroxide generation and lipid membrane peroxidation²³). For example, *Bcl-2* deficient mice (*Bcl-2* $-/-$) complete embryonic development and display relatively normal hematopoietic differentiation but demonstrate two potentially oxidation related abnormalities: polycystic kidney disease and hair hypopigmentation^{24,25}).

In short, based on findings of the above-mentioned studies, the increment of IL-3 increases Bcl-2 protein, which in turn switches off apoptosis and lipid membrane peroxidation. Decrement of IL-3, however, decreases Bcl-2 protein, which in turn switches on apoptosis and lipid membrane peroxidation.

Concerning NO production, however, a recent study showed that tumor-associated macrophages (TAMs) from within FSAN-JmIL3 tumors (fibrosarcoma transduced to express full-length mIL-3 cDNA) had decreased expression of TNF- α and iNOS, but that in short-term culture, TAMs regained their capacity to produce TNF- α and NO⁸). Therefore, our result that IL-3 itself increased NO production in diaphragm muscle fibers is consistent with this report. Regarding IL-3 involvement in antioxidant activity and NO production, we speculate that IL-3 induced NO production cause greater critical cellular damage than that resulting from antioxidant activity, resulting in diaphragm muscle deterioration by IL-3 per se.

It is noteworthy that IL-3 resulted in different responses of diaphragm muscle fibers with or without endotoxin. There have been two opposite reports regarding synergistic activity between IL-3 and endotoxin (LPS) in macrophages. A synergistic effect was found that IL-3 significantly enhanced the secretion of IL-1, IL-6 and TNF- α by LPS-stimulated macrophages. This synergistic activity of IL-

3 was observed over a wide range of *Escherichia coli* or *Salmonella enteritidis* LPS concentrations. Thus, IL-3 can potentiate the inflammatory response induced by endotoxin from Gram-negative bacteria through a potentiation of cytokine production²⁶). An antagonistic inhibition, however, was reported that the inhibitory effects of TNF- α , IFN- γ , or LPS were also seen when granulocyte-macrophage-CSF or IL-3 was used to stimulate bone marrow-derived macrophage (BMM) DNA synthesis²⁷). Our results seem to correspond to the latter report since we observed a partial antagonistic inhibition of IL-3 and endotoxin in diaphragm muscle fibers, not in macrophages.

In conclusion, the production of NO and the partial antagonistic inhibition of IL-3 and endotoxin seem to be strongly related to muscle contractile properties, that is, NO production can induce diaphragm muscle deterioration while the combination of IL-3 and endotoxin can prevent it. The present findings for IL-3 seem to be very similar to those of a previous report on IL-12¹²). We suggest, therefore, that there are two types of cytokines, namely, Th1-derived and Th2-derived cytokines, and the former which causes diaphragm muscle deterioration²⁸), and the later which prevents such deterioration²⁹). Furthermore, while Th1-derived cytokines induce diaphragm muscle deterioration, they have a cell protecting effect coexisted with endotoxin to prevent diaphragm muscle deterioration as is the case with IL-12 and IL-3. We consider this cell protecting effect to be an interesting phenomenon in the septic model, and speculate that it may have therapeutic potential for treatment of respiratory muscle failure due to septic shock.

Acknowledgments

The authors wish to thank Thomas Man-

deville for his review of the English in this paper. This study was supported in part by a grant from the Ministry of Education, Science, Sports and Culture of Japan (No. 12670545).

References

- 1) Fung, M.C., Hapel, A.J., Ymer, S., Cohen, D.R., Johnson, R.M., Campbell, H.D., Young, I.G.: Molecular cloning of cDNA for murine interleukin-3, *Nature*, **307**, 233-237, 1984
- 2) Ihle, J.N., Keller, J., Oroszlan, S., Henderson, L.E., Copeland, T.D., Fitch, F., Prystowsky, M. B., Goldwasser, E., Schrader, J.W., Palaszynski, E., Dy, M., Lebel, B.: Biologic properties of homogeneous interleukin 3. I. Demonstration of WEHI-3 growth factor activity, mast cell growth factor activity, P cell-stimulation factor activity, colony-stimulating factor activity, and histamine-producing cell-stimulating factor activity, *J. Immunol.*, **131**, 282-287, 1983
- 3) Rennick, D.M., Lee, F.D., Yokota, T., Arai, K.-I., Cantor, H., Nabel, G.J.: A cloned MCGF cDNA encodes a multilineage hematopoietic growth factor: Multiple activities of interleukin 3, *J. Immunol.*, **134**, 910-914, 1985
- 4) Teramura, M., Katahira, J., Hoshino, S., Motoji, T., Oshimi, K., Mizoguchi, H.: Clonal growth of human megakaryocyte progenitors in serum-free cultures: Effect of recombinant human interleukin 3, *Exp. Hematol.*, **16**, 843-848, 1988
- 5) Palacios, R., Henson, G., Steinmetz, M., McKearn, J.P.: Interleukin-3 supports growth of mouse pre-B-cell clones *in vitro*, *Nature*, **309**, 126-131, 1984
- 6) Palacios, R., Kiefer, M., Brockhaus, M., Karjalainen, K., Dembc, Z., Kisielow, P., Boehmer, H.: Molecular, cellular, and functional properties of bone marrow T lymphocyte progenitor clones, *J. Exp. Med.*, **166**, 12-32, 1987
- 7) Miyajima, A., Miyatake, S., Schreurs, J., Vries, J.D., Arai, N., Yokota, T., Arai, K.: Coordinate regulation of immune and inflammatory responses by T cell-derived lymphokines, *FASEB J.*, **2**, 2462-2473, 1988
- 8) Wu, Y.Z., Hong, J.H., Huang, H.H., Dougherty, G.J., McBride, W.H., Chiang, C.S.: Mechanisms mediating the effects of IL-3 gene expression on tumor growth, *J. Leukoc. Biol.*, **68**, 890-896, 2000
- 9) Lloyd, C.M., Gonzalo, J.-A., Nguyen, T., Delaney, T., Tian, J., Oettgen, H., Coyle, A.J., Gutierrez-Ramos, J.-C.: Resolution of bronchial hyperresponsiveness and pulmonary inflammation is associated with IL-3 and tissue leukocyte apoptosis, *J. Immunol.*, **166**, 2033-2040, 2001
- 10) Shi, Y., Wang, R., Sharma, A., Gao, C., Collins, M., Penn, L., Mills, G.B.: Dissociation of cytokine signals for proliferation and apoptosis, *J. Immunol.*, **159**, 5318-5328, 1997
- 11) Rinaudo, M.S., Su, K., Falk, L.A., Haldar, S., Mufson, R.A.: Human interleukin-3 receptor modulates *bcl-2* mRNA and protein levels through protein kinase C in TF-1 cells, *Blood*, **86**, 80-88, 1995
- 12) Nakahata, E., Shindoh, Y., Takayama, T., Shindoh, C.: Interleukin-12 prevents diaphragm muscle deterioration in a septic animal model, *Comp. Biochem. Physiol.*, **130**, 653-663, 2001
- 13) Shindoh, C., Hida, W., Ohkawara, Y., Yamauchi, K., Ohno, I., Takishima, T., Shirato, K.: TNF- α mRNA expression in diaphragm muscle after endotoxin administration, *Am. J. Respir. Crit. Care. Med.*, **152**, 1690-1696, 1995
- 14) Dawson, T.M., Bredt, D.S., Fotuhi, M., Hwang, P.M., Snyder, S.H.: Nitric oxide synthase and neuronal NADPH diaphorase are identical in brain and peripheral tissues, *Proc. Natl. Acad. Sci. USA*, **88**, 7797-7801, 1991
- 15) Dubowitz, V., Brooke, M.H.: Histological and histochemical stains and reactions. *In* Dubowitz, V., Brooke, M.H., editors. *Muscle Biopsy: A modern approach*. W.B. Saunders Company Ltd, London-Philadelphia-Toronto. 20-33, 1973
- 16) Close, R.I.: Dynamic properties of mammalian skeletal muscles, *Physiol. Rev.*, **52**, 129-197, 1972
- 17) Kobzik, L., Reid, M.B., Bredt, D.S., Stamler, J.S.: Nitric oxide in skeletal muscle, *Nature*, **372**, 546-548, 1994

IL-3 Effect on Diaphragm Muscle

- 18) Geng, Y., Hansson, G.K., Holme, E. : Interferon-gamma and tumor necrosis factor synergize to induce nitric oxide production and inhibit mitochondrial respiration in vascular smooth muscle cells, *Circ. Res.*, **71**, 1268-1276, 1992
- 19) Gillessen, S., Mach, N., Small, C., Mihm, M., Dranoff, G. : Overlapping roles for granulocyte-macrophage colony-stimulating factor and interleukin-3 in eosinophil homeostasis and contact hypersensitivity, *Blood*, **97**, 922-928, 2001
- 20) Pulaski, B.A., McAdam, A.J., Hutter, E.K., Biggar, S., Lord, E.M., Frelinger, J.G. : Interleukin 3 enhances development of tumor-reactive cytotoxic cells by a CD4-dependent mechanism, *Cancer Res.*, **53**, 2112-2117, 1993
- 21) Strasser, A., Whittingham, S., Vaux, D.L., Bath, M.L., Adams, J.M., Cory, S., Harris, A.W. : Enforced *BCL2* expression in B-lymphoid cells prolongs antibody responses and elicits autoimmune disease, *Proc. Natl. Acad. Sci. USA*, **88**, 8661-8665, 1991
- 22) Kluck, R.M., Bossy-Wetzell, E., Green, D.R., Newmeyer, D.D. : The release of cytochrome c from mitochondria : A primary site for Bcl-2 regulation of apoptosis, *Science*, **275**, 1132-1136, 1997
- 23) Hockenbery, D.M., Oltvai, Z.N., Yin, X.-M., Millman, C.L., Korsmeyer, S.J. : Bcl-2 functions in an antioxidant pathway to prevent apoptosis, *Cell*, **75**, 241-251, 1993
- 24) Veis, D.J., Sorenson, C.M., Shutter, J.R., Korsmeyer, S.J. : Bcl-2-deficient mice demonstrate fulminant lymphoid apoptosis, polycystic kidneys, and hypopigmented hair, *Cell*, **75**, 229-240, 1993
- 25) Korsmeyer, S.J., Shutter, J.R., Veis, D.J., Merry, D.E., Oltvai, Z.N. : Bcl-2/Bax : a rheostat that regulates an anti-oxidant pathway and cell death, *Semin. Cancer Biol.*, **4**, 327-332, 1993
- 26) Cohen, L., David, B., Cavaillon, J.M. : Interleukin-3 enhances cytokine production by LPS-stimulated macrophages, *Immunol. Lett.*, **28**, 121-126, 1991
- 27) Vairo, G., Argyriou, S., Knight, K.R., Hamilton, J.A. : Inhibition of colony-stimulating factor-stimulated macrophage proliferation by tumor necrosis factor-alpha, IFN-gamma, and lipopolysaccharide is not due to a general loss of responsiveness to growth factor, *J. Immunol.*, **146**, 3469-3477, 1991
- 28) Shindoh, C., Katayose, D., Shindoh, Y., Shirato, K. : Effects of interleukin-8 on diaphragm muscle contraction in rats, *Bull. Coll. Med. Sci. Tohoku Univ.*, **10**, 135-144, 2001
- 29) Taneda, A., Shindoh, C., Ohuchi, Y., Shirato, K. : Protective effects of interleukin-10 on diaphragm muscle in a septic animal model, *Tohoku J. Exp. Med.*, **185**, 45-54, 1998